MULTITONE NONLINEAR CODING

ANDRZEJ NOWICKI, JANUSZ WÓJCIK, WOJCIECH SECOMSKI

Institute of Fundamental Technological Research of Polish Academy of Sciences
Świętokrzyska 21, 00-049 Warsaw, Poland
anowicki@ippt.gov.pl

A new method that utilizes nonlinear properties of tissue (or another media) to improve ultrasound image resolution is presented. In our novel method the acoustic source is activated with two tones burst (2.2 and 4.4 MHz) with specially designed polarization of the individual tone burst. This new approach is called multi tone nonlinear coding MNC because the choice of polarization of the both tones (and their amplitudes) allowing optimization of the receiving properties depends on the nonlinear properties of tissue. The calculations were done for two tones bursts propagating in the tissue-like lossy medium with absorption of 7 Np/m·MHz. The concept of the Virtual Fields was introduced to explain abilities and properties of pulse inversion and MNC method and to compare both. Comparison of the spatial field distribution obtained using MNC and conventional harmonic imaging approach, in which the first harmonic is used to reconstruct the image are presented.

INTRODUCTION

A new US modality called Tissue Harmonic Imaging (THI) was first described by Averkiou et al in 1997, [1]. Nowadays, this technique is routinely used in ultrasonic imaging proving its importance in improved quality of grey-scale images, especially in examining of the so-called "difficult patients", [3, 7]. However, it has to be stressed that it is far from optimal because only half of the available transducer bandwidth is used for image formation – lower half for transmission and upper half during reception. The importance of the reduced dynamic range and penetration encountered in THI was also pointed out [1, 2]. Since the images are formed with only the first harmonic components which are usually at least 20 dB below the fundamental the dynamic range is limited. The nonlinear effects including contrast agents improving the imaging sensitivity was intensively studied by many authors, (eg. [4, 5].

An improved resolution can be achieved with an imaging method called pulse inversion (PI). In contrast to conventional harmonic imaging, for pulse inversion imaging the whole frequency spectrum can be used during reception. Alternate pulses, π radians out of phase, are transmitted along the same scan line, [6]. The echoes received from the pair transmission are then summed to build up the final image line. This method removes the requirement of

narrow band transmitting for harmonic signal extraction and even in the case of broadband transmitting where fundamental and harmonic components overlap, the harmonic component can be extracted.

We are proposing a novel method termed Multitone Nonlinear Coding (MNC) that through the utilizing of the nonlinear acoustic properties of tissue can improve: ultrasound image resolution and signal to noise ratio for mechanical index (MI) lower than for PI method. PI is considered here as a reference method.

1. NONLINEAR MODEL

In the description of the phenomena building the foundations of both method, PI and MNC we have been solving second order nonlinear partial differential equation describing the model in dimensionless system of units]8[.

$$\Delta P - \partial_{tt} P - 2\partial_t \mathbf{A}P = -q\beta\partial_{tt}\left(P\right)^2 \qquad (1)$$
$$\mathbf{A}P \equiv A(t) \otimes P(\mathbf{x},t),\ A(t) = F^{-1}\left[a(n)\right]$$

where; $P(\mathbf{x},t)$ is the pressure in space coordinates $\mathbf{x}$ and time t; $\mathbf{A}$ is a convolution type operator describing the absorption; q is the Mach number (for velocity on source surface); $\beta \equiv (\gamma+1)/2; \gamma \equiv (B/A)+1$, or γ - exponent of the adiabate; $n \equiv f/f_0$ - dimensionless frequency, f, f_0 - frequency and characteristic frequency subsequently; $a(n)$ - small signal absorption coefficient, $\mathbf{A} = \mathrm{F}^{-1}\left[a(n)\right]$, $\mathrm{F}[\cdot]$ - Fourier transform. The most important properties of the model resulting from the nonlinear properties of tissue are as follows. If $P^+(\mathbf{x},t)$ is a solution of the linear propagation equation ($q \equiv 0$) fulfilling the boundary condition $P^+(\mathbf{x},t) = P^+(S(\mathbf{x}),t)$ for $\mathbf{x} \in S(\mathbf{x})$, where $S(\mathbf{x})$ is the surface of the source, then $P^-(\mathbf{x},t) \equiv -P^+(\mathbf{x},t)$ is also the solution of the same equation for boundary condition with reverse phase $P^-(S(\mathbf{x}),t) = -P^+(S(\mathbf{x}),t)$ and $P^+(\mathbf{x},t) + P^-(\mathbf{x},t) = 0$. For non-linear propagation ($q \neq 0$) $P^+ + P^- \neq 0$ despite the fact that $P^+(S(\mathbf{x}),t) + P^-(S(\mathbf{x}),t) \equiv 0$.

All the results of numerical calculations that are presented in this paper have been obtained by means of the previously developed solver [10]. The boundary conditions were assumed as for a spherically focusing circular transducer with the diameter of 12.8 mm and geometrical focus $z_g = 60$ m. For axially symmetrical fields $\mathbf{x} \equiv (r,z)$, $r \equiv \sqrt{x^2+y^2}$ is the radial coordinate, z is the coordinate along beam axis. The profiles for time-relating excitations relevant for the analyzed cases are presented later in this paper. Finally, the non-linear medium was assumed with $\gamma = 6$ and absorption coefficient $\alpha_1 = 7$ Np/mMHz. The peak pressure amplitude on transducer surface $S(\mathbf{x})$ -was equal to $P_{max} = 0.5$ MPa.

2. PULSE INVERSION METHOD

Here we are briefly recalling the basic idea of the PI method. We consider PI as a reference method well established in clinical ultrasonography. The Eq.(2) describes two pulses with opposite phase, transmitted one after another. As can be seen, the sum of the initial pulses is equal to zero.

$$P_{\mathrm{PI}}(t,\mathbf{x}) \equiv \begin{Bmatrix} +1 \\ or \\ -1 \end{Bmatrix} \cdot \sin(\omega_1 t) \cdot \mathrm{Env}(t) \Rightarrow \begin{cases} P_{po}(t,\mathbf{x}) \\ P_{mo}(t,\mathbf{x}) \end{cases} \quad \mathbf{x} \in S(\mathbf{x}) \tag{2}$$

where; $\omega_1 = 2\pi \cdot f_1$ is the pulsation, f_1 is carrier frequency, $\mathrm{Env}(t)$ is pulse envelope. The positive polarization +**1** is marked here with subscript *p* and negative polarization -**1** is marked with subscript *m*.

Although the moduli of the Fourier spectra of the transmitted pulses (2) are identical - see Fig.1.a. - but their polarization phases are opposite.

$$\left|F_{p0}(f,\mathbf{x})\right| = \left|F_{m0}(f,\mathbf{x})\right|,\ F_{p0}(f,\mathbf{x}) \equiv \mathrm{F}\left[P_{p0}(t,\mathbf{x})\right] = -\mathrm{F}\left[P_{m0}(t,\mathbf{x})\right],\ \mathbf{x} \in S(\mathbf{x}) \tag{3}$$

The nonlinear medium differentiates the initial polarization of the propagating pulses. The resulting differences in amplitude and phase can be exhibit by the sum of the pressure fields of the incident pulses $P_{p0}^{in}(t,\mathbf{x})$, $P_{m0}^{in}(t,\mathbf{x})$ or their Fourier spectra in any point $\mathbf{x}$ of the medium

$$F_{p0m0}(f,\mathbf{x}) \equiv F_{p0}(f,\mathbf{x}) + F_{m0}(f,\mathbf{x}), \tag{4}$$

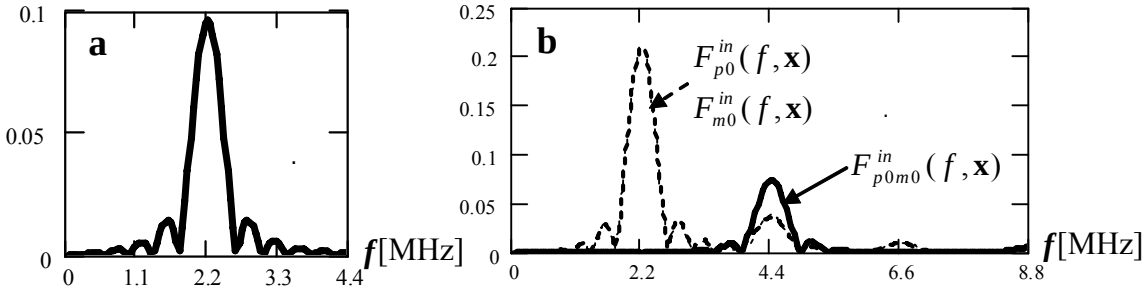

Fig.1 Moduli of the Fourier spectra for the PI method. (a) Fourier spectra of the pulses from the Eq.(2). (b) Results of nonlinear propagation of pulses as in Eq.(2) for PI -near physical focus **x**=(0mm; 40mm). $F_{p0}(f,\mathbf{x}), F_{m0}(f,\mathbf{x})$-module of Fourier spectra of incident pulses-dashed lines; $F_{p0m0}(f,\mathbf{x})$-modulus of the sum of Fourier spectra of incident pulses -solid

Fig. 1.b. shows the results of the propagation of pulses transmitted one by one to the medium. The dashed lines represent moduli of their Fourier spectra on the beam axis at $r = 0$ and $z = 40\,\mathrm{mm}$ (near physical focus $\mathbf{x}_{ph} \cong (0;33\mathrm{mm})$). The carrier frequency was equal $f_1 = 2.2\,\mathrm{MHz}$. The solid line represents the modulus of the resulting Fourier spectrum $\left|F_{p0m0}(f,\mathbf{x})\right|$. As can be observed, the Fourier components of both pulses near f_1 practically cancel each other in the absorbing media. The differences in amplitude and phase of the incident pulses cause the differences in scattered fields $P_{p0}(t,\mathbf{x})$, $P_{m0}(t,\mathbf{x})$ and in their Fourier spectra $F_{p0}(f,\mathbf{x}), F_{m0}(f,\mathbf{x})$ which can be exposed (formally) in the same way like to incident fields

$$F_{p0m0}(f,\mathbf{x}) \equiv F_{p0}(f,\mathbf{x}) + F_{m0}(f,\mathbf{x}). \tag{5}$$

Accordingly to the above observation, the resulting differences in amplitude and phase of the received echoes can be enhanced by the sum of the detected signals $P_{p0}(t)$, $P_{m0}(t)$ ($F_{p0}(f)$,$F_{m0}(f)$)

$$P_{p0mo}(t) \equiv P_{p0}(t) + P_{m0}(t) \tag{6}$$

3. THE BASE OF MNC METHOD

The formula below explains how four different pulses can be encoded through the choice of polarization of two individual tones.

$$P_{\mathrm{NC}}(t,\mathbf{x}) \equiv \left\{ \begin{matrix} +\mathbf{1} & +\mathbf{1} \\ or \cdot \sin(\omega_1 t) + or \cdot \sin(\omega_2 t - \varphi) \\ -\mathbf{1} & -\mathbf{1} \end{matrix} \right\} \cdot \mathrm{Env}(t) \Rightarrow \left\{ \begin{matrix} P_{pp}(t,\mathbf{x}) \\ P_{pm}(t,\mathbf{x}) \\ P_{mp}(t,\mathbf{x}) \\ P_{mm}(t,\mathbf{x}) \end{matrix} \right., \quad \mathbf{x} \in S(\mathbf{x}) \tag{7}$$

where: $\omega_2 = 2\omega_1$ and φ - relative phase, here $\varphi = 0$. In the MNC method, the first contributing tone has a fundamental pulsation ω_1 and the pulsation of the second one is doubled. It means that the transmitted pulses have initially two frequencies; fundamental f_1 and harmonic $f_2 \equiv 2 \cdot f_1$. Each of the tones has its own polarization see Fig.2.a. and Fig.2.b.

Results of nonlinear propagation: Although the moduli of the spectra of the transmitted pulses are two by two identical -see Fig.2.b. - but the polarizations of the individual tones are different within each pair. According to a general comment following Eq.(1) even if $P_{pp} = -P_{mm}$, $P_{pm} = -P_{mp}$ and $F_{pp} = -F_{mm}, F_{pm} = -F_{mp}$ on the source ($\mathbf{x} \in S(\mathbf{x})$), then under the condition of nonlinear propagation in tissue four different pulses $P_{pp} \neq -P_{mm} \neq P_{pm} \neq -P_{mp}$ and $F_{pp} \neq -F_{mm} \neq F_{pm} = -F_{mp}$ are obtained for $\mathbf{x} \notin S(\mathbf{x})$ (provided for z is large enough).

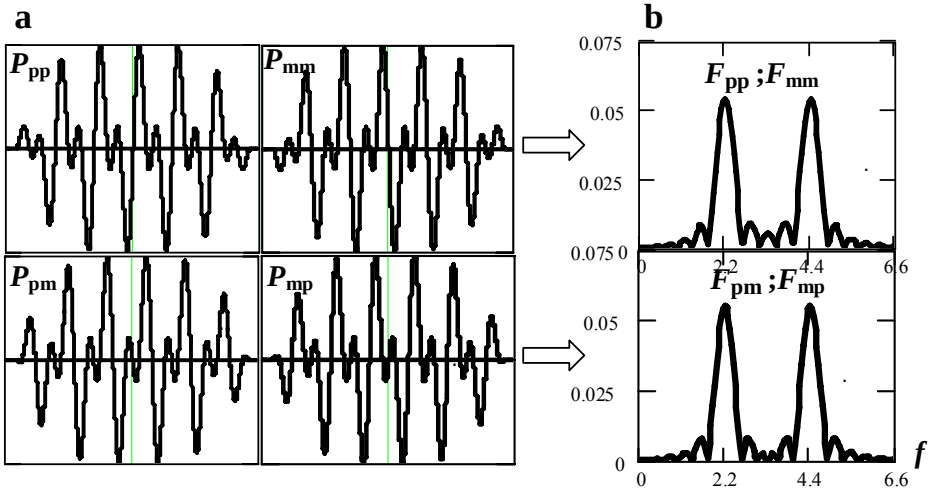

Fig.2 (a) Examples of four pulses which encoded according to Eq.(4) in the MNC method. All pulses where normalized to 1. (b) The pair of the moduli of Fourier spectra for the initial pulses, f - in MHz

Pulses combination in MNC: In case of PI we had to deal with only one pair of pulses and the only one interrelation between polarizations of the pulses within the pair – opposite one to another. Therefore the transmission scheme was obvious. By applying the above rule to our case, with restriction that only two pulses can be combined, we conclude that four basic pulses make it possible to create six following pairs of pulses that meet the above requirement: $\left[P_{pp}, P_{mm}\right], \left[P_{pm}, P_{mp}\right], \left[P_{pp}, P_{mp}\right], \left[P_{pm}, P_{mm}\right], \left[P_{pp}, P_{pm}\right], \left[P_{mm}, P_{mp}\right]$.

As a result of non-linear propagation of every pulse within the common pair, detection of scattered signals with subsequent addition or subtraction of the two echo signals, the result, where the nonlinear effects are accentuated or amplified at the bands of higher frequencies $2f_1, 3f_1$ is obtained. With respect to incident (*in*) and scattered (*sc*) fields as well as the signals that are detected by the receiver (*e*), the combination of pulses within the relevant pairs are as follows:

$$\begin{aligned} P_{ppmm} &\equiv P_{pp} + P_{mm}, \quad & P_{pmmp} &\equiv P_{pm} + P_{mp}, \\ P_{ppmp} &\equiv P_{pp} + P_{mp}, \quad & P_{pmmm} &\equiv P_{pm} + P_{mm}, \\ P_{pppm} &\equiv P_{pp} - P_{pm}, \quad & P_{mmmp} &\equiv P_{mm} - P_{mp}, \end{aligned} \tag{8}$$

In the same way the combinations of spectral representations for pulse pairs can be presented. It should be taken into consideration that the two upper pairs of pulses in Eq.8 that produce combinations P_{ppmm} and P_{pmmp} (F_{ppmm}, F_{pmmp}) comprise pulses with opposite polarization. These two special cases of MNC are referred to as the multitone pulse inversion (MPI). In these two cases not only harmonics for the fundamental MNC tone are amplified, but also the second harmonics for the fundamental tone are created and subject to amplification $f_3 = 3 \cdot f_1$. Under specific conditions these upper harmonics can be also detected. Anyway, it should be noted that $P_{(....)}(t,\mathbf{x}), P_{(....)}(t,\mathbf{x})$ are not tangible physical objects that really exist but they present rather virtual structures, as the fields that contribute formation of these objects do not co-exist in the medium.

4. VIRTUAL FIELDS

The concept of the virtual incident and backscattered fields allows us to explain some properties (improved resolution, reduction of side lobes, SNR gain) and conduct the comparison of both PI and MNC methods. Let's consider the excitation of the transducer with $P_{pp}(t)$ and $P_{mm}(t)$ pulses, transmitted one after another along the scan line (Fig.3.a.). Despite the difference of the pulses for PI and MNC, the excitation and detection schemes are identical.

Each has its own acoustical pressure field distribution. Because (for single pulses) $P_{(1)}(t,\mathbf{x}) \neq 0$ for $t_1 \le t \le t_1 + t_{dur}$ and $P_{(2)}(t,\mathbf{x}) \neq 0$ for $t_2 \le t \le t_2 + t_{dur}$ for $t_1 + t_{dur} \le t_2$ where, t_1, t_2 are the starting times of the first and second pulse respectively, t_{dur} is the duration of the pulse, then these pulses are not coexisting simultaneously in the medium and then they are not generating the real acoustical field representing their superposition. However, the superposition of the individual pulses propagating separately can be easily done in the computer in the common operation time *t* or after detection and delay by $\delta t = t_2 - t_1$.

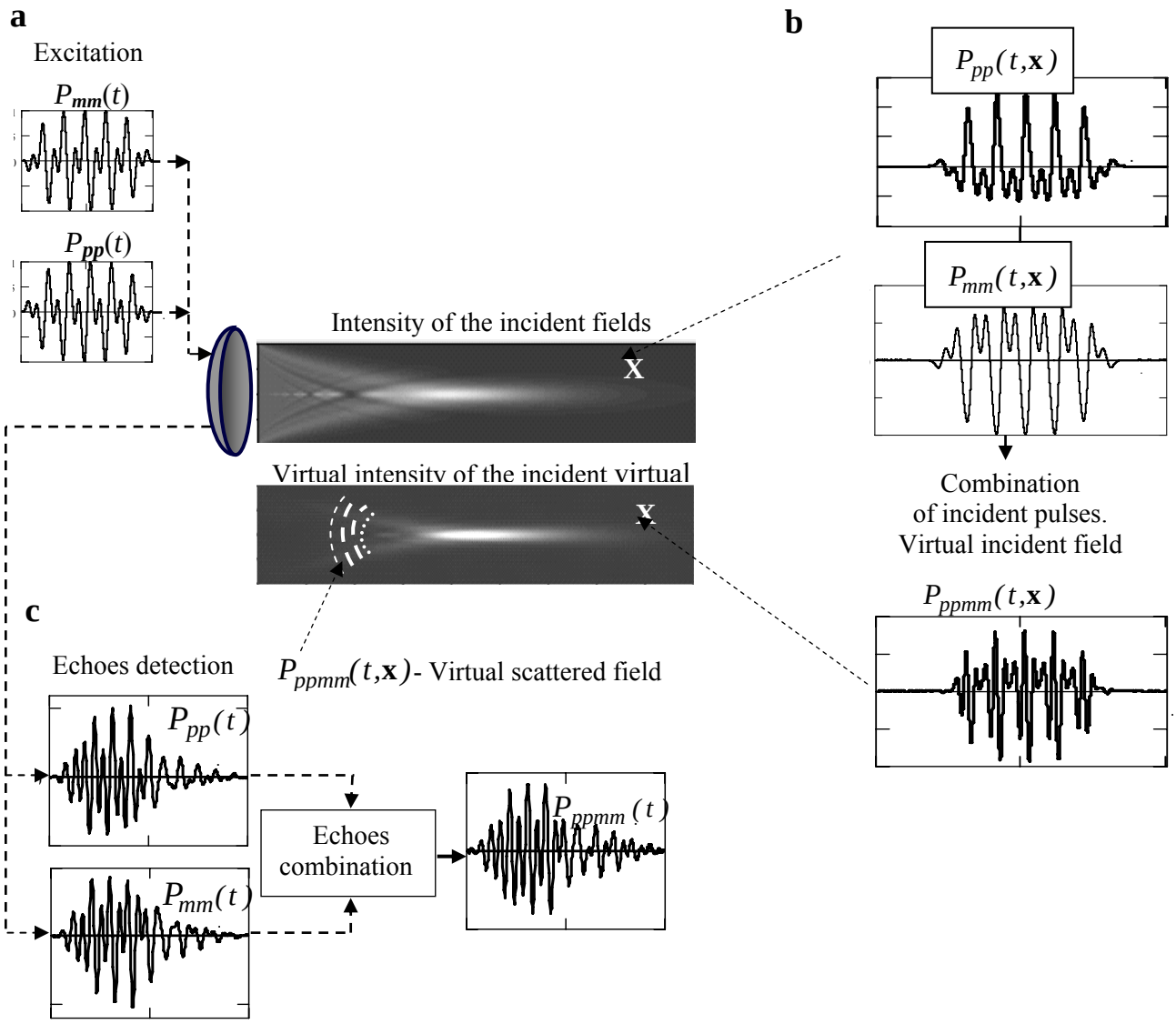

Fig.3 Concept of the virtual fields. (a) original excitation pulses. (b) Propagated incident pulses $P_{pp}(t,\mathbf{x})$, $P_{mm}(t,\mathbf{x})$ (top plots) and distribution of their intensities $I_{pp}(\mathbf{x})$ ($I_{mm}(\mathbf{x})$) (in center on the top). Combination of the propagating pulses resulting in final virtual incident pulse $P_{ppmm}(t,\mathbf{x})$ (down) and their virtual intensity $I_{ppmm}(\mathbf{x})$ (center down). (c) Detected echoes

When both incident pulses are combined together, the final virtual pulse is obtained. The corresponding spatial field distribution is called the incident virtual field. An example of the virtual intensity $I_{ppmm}(\mathbf{x})$ of the virtual incident field $P_{ppmm}(t,\mathbf{x})$ for two pulses $P_{pp}(t,\mathbf{x})$ and $P_{mm}(t,\mathbf{x})$ is shown in Fig.3.b.

Hereafter the examples for spatial distribution of Fourier spectra shall be presented, but for only one specific frequency. Properties of incident pulses and their combination as well as the effect of implementation of the compensation rule for the space can be illustrated by means of componential spatial distributions for Fourier spectrum for incident pulses and for a virtual incident pulse.

The resolution ability of both, MNC and PI methods is compared in Fig.4. On the upper-left we can see the intensity field for one of the pulses P_{p0} transmitted in PI and for one pulse P_{pp} out of four in MNC. The lateral beam width is plotted along the dashed white line that is clearly narrower than in case when two tones are transmitted-solid line.

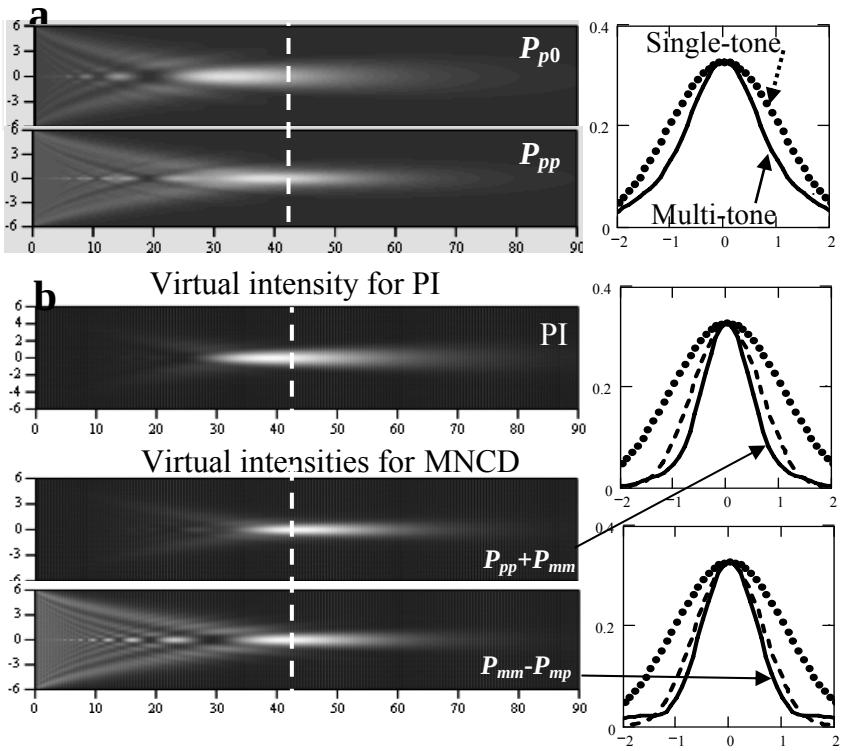

Fig.4 (a) Intensities for the single-tone and two-tones pressure fields applicable to PI and MNC methods. (b) Intensities for virtual fields calculated for PI (upper image) and two cases of MNC (middle and bottom). The corresponding cross-sections of the intensity fields at the distance of 43 mm from the transducer are plotted on the right. (right plots) the dotted lines correspond to the intensities of a single-tone burst; the dashed lines correspond to virtual intensity in PI. Scale in [mm]

The mechanical indices (MI) and ratios of the emitted energies E, intensities I and resolution (Res) ratio for direct transmission in the tissue for original pulses used in PI and our method were as follows:

$$\frac{\mathrm{MI_{PI}}}{\mathrm{MI_{MNC}}} = \frac{0.216}{0.134} \cong 1.61, \quad \frac{I_{\mathrm{PI}}(\mathbf{x})}{I_{\mathrm{MNC}}(\mathbf{x})} > \frac{\mathrm{E_{PI}}}{\mathrm{E_{MNC}}} = 1.65 , \qquad \frac{\mathrm{Res_{MNC}}}{\mathrm{Res_{PI}}} \approx 1.3 .$$

It should be noticed that MI for PI is by more than 60% higher than for MNC.

The ratios of intensities, calculated for virtual fields intensities, for two cases of MNC (Multitone Pulse Inversion MPI) and other cases and for resolution ratios for **virtua**l fields equaled to;

$$\frac{I_{\mathrm{MNC(MPI)}}}{I_{\mathrm{PI}}} \cong 0.63 , \quad \frac{I_{\mathrm{MNC}}}{I_{\mathrm{PI}}} \cong 6, \qquad \frac{\mathrm{Res_{MNC}}}{\mathrm{Res_{PI}}} \cong 1.1 \div 1.3 .$$

The first ratio stands for the decrease of the virtual energy while the second one shows that the virtual energy increases. The increase of the ratio of the virtual field intensities indicates the advantage of the new method, the gain in the echoes is reached without any additional thermo-mechanical effects.

5. EXPERIMENTS

The experimental set-up consisted of a PC computer with software for programming the required scanning pulses according to Eq.(2) and Eq.(7). Signals from the computer drove the Signal Synthesizer (HP8643A, Agilent, USA). After amplification in the power RF amplifier (ENI 3100LA, USA) the transmitter bursts excited the ultrasonic transducer (geometrical focus z_g =60 mm, diameter = 12.8 mm, bandwidth =65%). The generated pulses had initially four periods for 2.2 MHz. However, the real transmitted pulse had nearly 6 periods due to the ringing effect of the transducer. To check whether the transmitted pulses matched the anticipated properties for both MNC and PI we carefully measured the pressure fields generated by these pulses, with the PVDF hydrophone (Sonora Medical Systems model Sonic 804-201, USA). Transmitted pulse for PI (upper) and MNC (middle and bottom) and their Fourier spectra (left) measured near the transducer face, Fig.5.

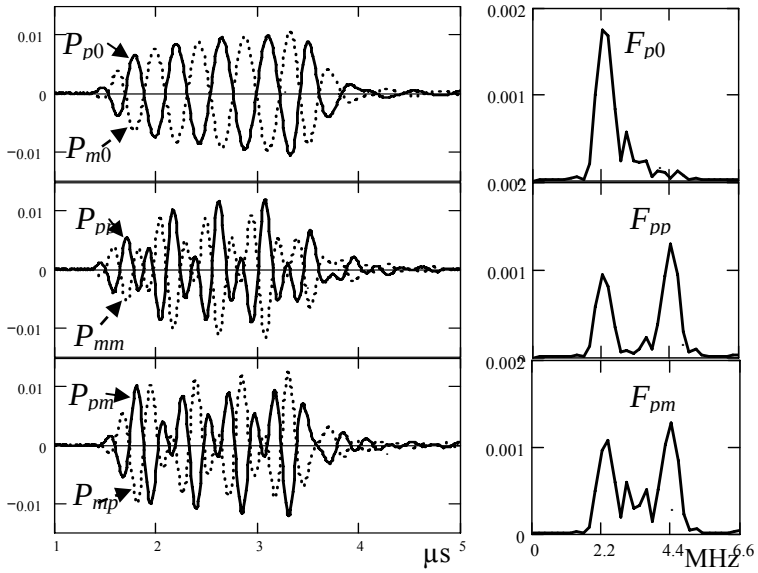

Fig.5 Transmitted pulse for PI (upper) and MNC (middle and bottom) and their Fourier spectra (left) measured near the transducer face

The produced pulses perfectly fulfilled the required symmetry for pairs of opposite polarization. Their amplitudes were identical. The amplitude of pulses used for PI was about 4% lower than the one for MNC, advantageous for lower MI for PI, and even then the MI for PI was by almost 60% higher than for MNC. The emitted energies were also always higher for PI, by 40% comparing to P_{pp} and P_{mm} and by 13% when constructing P_{pm} or P_{mp} pulses.

In the following experiment three cotton threads stretched in water (very low absorption) were scanned using both, PI and MNC methods. The positioning of threads in the scanning field is shown schematically in Fig.6a. in the left upper corner – however the proportions between dimensions of the beam and the target are not obeyed. The beam is directed perpendicularly to the planes where the threads are positioned. Cross-section of filaments as cut by the scanning beam plane were considered as polygons – i.e. they had edges and lateral planes with various inclination angles with respect to the scanning beam. The scan probe displacement step in x direction was δx =0.2 mm over the range from 0 mm to

9mm. The central thread in the phantom is positioned approximately for scan position $x \cong 4.5$mm and 40mm from the transducer.

Three pairs of plots in Fig.6b. serve as the comparison of signals for lines vs. the scanning co-ordinate x. The plots were derived from virtual echoes for PI and for three cases of MNC in accordance with he formula Eq.(10) for t=2.33μs (= 3.5mm). The solid lines are plotted for MNC (three cases marked by pmmp, mmpm, mmmp) recorded along the solid white line on Fig.6c. The dashed lines are plotted for PI recorded along the dashed white line (at the same depth). The images show that inferior resolution of PI results in errors of relative location of targets – it is explained by the influence of signals from the neighboring target (the overlapping results in offset of maximums for side targets).

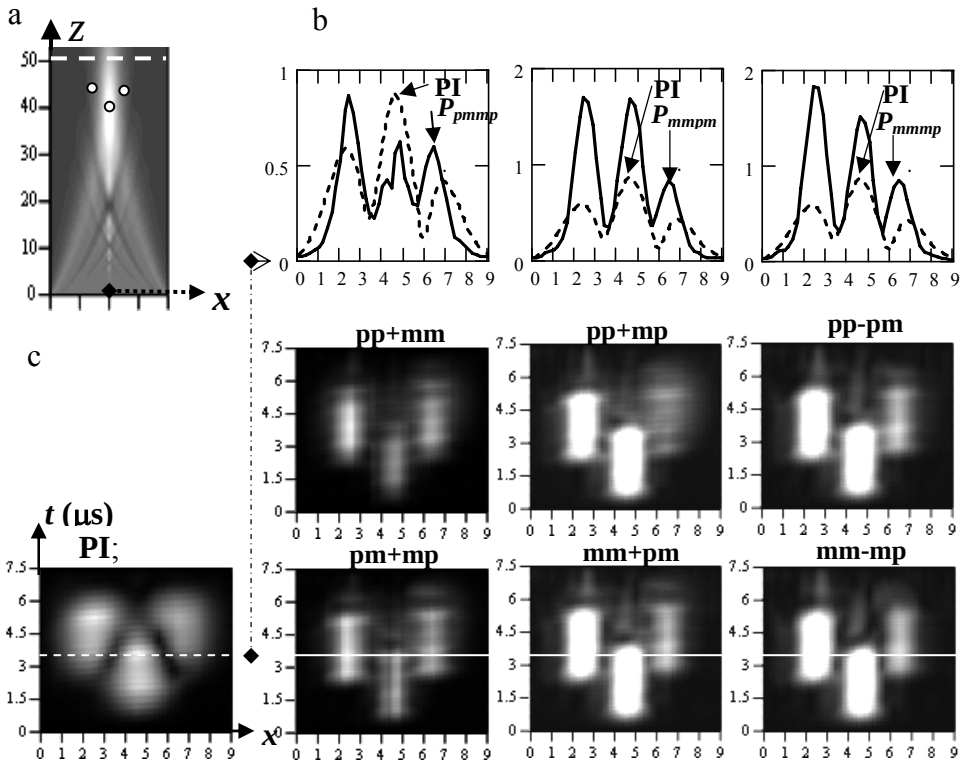

Fig.6 Comparison of PI and MNC for three threads in water as the target. (a) Scan configuration. (b) Comparison PI –dashed lines and three cases of MNC –solid lines for the lateral section along lines- dashed for PI and solid for MNC- in figure (c). Horizontal scales in mm

6. DISCUSSION

In conventional harmonic imaging a single tone burst is applied to the acoustic source and then the first harmonic echo is extracted to generate the tissue images with presumably improved resolution. However, as it was mentioned before, the transmitting/receiving bandwidth and efficiency are used in insufficient way as only half of the bandwidth is occupied during transmission. This is the case for both, standard harmonic imaging and PI technique. In the novel multitone (two harmonic tones in the case reported) coding full available bandwidth is employed during transmission and reception.

Subsequently, for MNC the acoustic energy available for image construction can be even twofold larger with the corresponding increase in SNR as compared to the conventional harmonic imaging. In the description of the phenomena accompanying propagation of signals

used in harmonic imaging PI and MNC methods we have been solved the second order nonlinear partial differential equation describing the model in dimensionless system of units. Mechanical Index is lower for MNC in comparison to PI for the same initial peak to peak pressure; $MI_{PI}/MI_{MNC}= (0.214/0.134)\approx 1.61$

- Lateral resolution was better for MNC comparing to PI by the factor from 1.1 to 1.3
- Positioning of both the entire target and its components improved for even complex targets.
- In comparison to the Pulse Inversion this new approach allows to process six different decoding schemes of the received echoes (out of six two correspond to multitone PI)

In the media exhibiting strong absorption the amplitude ratio of MNC/PI was between 0.5 and 1 for signals P_{ppmm} and P_{pmmp} (here called MPI). For other four cases this ratio was between ~ 6 and 8. It should be noticed that the signal gain for MNC diminishes with decreasing absorption of the examined media. For water this ratio was equal to 1 and 2 respectively.

Depending on the processing scheme some different spectral components of the resulting spectra can be enhanced. This can result in optimal compensation or rejection of the fundamental component, leaving the first harmonic only or even transferring part of the received energy to the second harmonics.

ACKNOWLEDGMENTS

This work was supported by the Ministry of Science and Higher Education grant N5180023210219.

REFERENCES

1. M.A. Averkiou, D.R. Roundhill, J.E. Powers, A new imaging technique based on the nonlinear properties of tissues, in: Proc. IEEE Ultrason. Symp., Vol. 2, , pp. 1561–1566, 1997.
2. M.A. Averkiou, Tissue harmonic ultrasonic imaging, C. R. Acad. Sci., t. 2, Série IV, (Applied physics, Biophysics), 1139–1151, Paris 2001.
3. H. Becher, K. Tiemann, C. Pohl, N.C. Nanda, M.A. Averkiou, J.E. Powers, B. Luderitz, Improvement in endocardial border delineation using tissue harmonic imaging, Echocardiography, 15, 511–517, 1998.
4. T. Christopher, Experimental investigation of finite amplitude distortion-based second harmonic pulse echo ultrasonic imaging, IEEE Trans. Ultrason., Ferroelect., Freq. Contr., vol. 45, no. 1, pp. 158–162, 1998.
5. T. Christopher, Finite amplitude distortion-based inhomogeneous pulse echo ultrasonic imaging, IEEE Trans. Ultrason.Ferroelect., Freq. Contr., vol. 44, no. 1, pp. 125–139, 1997.
6. D. Simpson Hope, C.T. Chin, P.N. Burns, Pulse inversion doppler: A new method for detecting nonlinear echoes from microbubble contrast agents, IEEE Trans. Ultrason. Ferr. Freq. Control, 46, 2, 372–382, 1999.
7. F. Tranquart, N. Grenier, V. Eder, L. Pourcelot, Clinical use of ultrasound tissue harmonic imaging, Ultrasound Med.Biol., vol. 25, no. 6, pp. 889–894, 1999.
8. J. Wójcik, Conservation of energy and absorption in acoustic fields for linear and nonlinear propagation, J.Acoust. Soc. Am., 104(5), 2654-2663, 1998.
9. J. Wójcik, Nonlinear reflection and transmission of plane acoustics waves, Archives of Acoustics, Vol.29,No 4, . 607-632, 2004.
10. J. Wójcik, A. Nowicki, P.A. Lewin, P.E. Bloomfield, T. Kujawska, L. Filipczynski, Wave Envelopes Method for Description of Nonlinear Acoustic Wave Propagation, Ultrasonics, 44, 3, 310-329, 2006.